Published in final edited form as:

Cancer Res. 2018 July 01; 78(13): 3458–3468. doi:10.1158/0008-5472.CAN-17-2296.

PSMD5 inactivation promotes 26S proteasome assembly during colorectal tumor progression

Avi Levin[1,2], **Adi Minis**[1], **Gadi Lalazar**[3], **Jose Rodriguez**[1], and **Hermann Steller**[1]

[1]Strang Laboratory of Apoptosis and Cancer Biology, The Rockefeller University, 1230 York Avenue, New York, NY 10065, USA

[2]Division of Gastroenterology, University of Iowa, Iowa City, IA 52242, USA

[3]Laboratory of Cellular Biophysics, The Rockefeller University, 1230 York Avenue, New York, NY, 10065, USA

Abstract

Protein degradation by the ubiquitin-proteasome system (UPS) is central to protein homeostasis and cell survival. The active 26S proteasome is a large protease complex consisting of a catalytic 20S subunit and 19S regulatory particles. Cancer cells are exposed to considerable protein overload due to high metabolic rates, reprogrammed energy metabolism and aneuploidy. Here we report a mechanism that facilitates the assembly of active 26S proteasomes in malignant cells. Upon tumorigenic transformation of the gut epithelium, 26S proteasome assembly was significantly enhanced, but levels of individual subunits were not changed. This enhanced assembly of 26S proteasomes increased further with tumor progression and was observed specifically in transformed cells, but not in other rapidly dividing cells. Moreover, expression of PSMD5, an inhibitor of proteasome assembly, was reduced in intestinal tumors and silenced with tumor progression. Re-expression of PSMD5 in tumor cells caused decreased 26S assembly and accumulation of poly-ubiquitinated proteins. These results suggest that inhibition of cancer-associated proteasome assembly may provide a novel therapeutic strategy to selectively kill cancer cells.

Keywords

tumor proteostasis; colorectal cancer; 26S proteasome; proteasome assembly; PSMD5; protein translation

Introduction

Protein synthesis and degradation are coordinated to allow adaptation to a rapidly changing microenvironment (1–3). Elevated protein synthesis can generate significant amounts of

Corresponding authors: Avi Levin. avraham-levin@uiowa.edu. University of Iowa Hospitals and Clinics. 200 Hawkins Drive, Iowa City, IA 52242, USA. Tel: (319)-356-7368. Hermann Steller. steller@rockefeller.edu. Strang Laboratory of Apoptosis and Cancer Biology, The Rockefeller University, 1230 York Avenue, New York, NY 10065, USA. Tel: (212) 327-7075.

Conflict of interest: A.L., A.M., J.R. and H.S. declare no conflicts of interest; G.L. has a significant financial interest in and receives compensation from Immuron Ltd. and Fortress Biotech Ltd. in projects unrelated to this work.

superfluous and damaged proteins. that are potentially toxic. However, cells can increase their rates of protein degradation to maintain protein homeostasis (4,5). Selective protein degradation plays central roles in multiple biological processes including removal of misfolded and potentially toxic proteins, control of cell-cycle progression, regulation of gene expression, and changes in cell size and morphology (6,7). The selective degradation of most intracellular proteins is carried out by the ubiquitin-proteasome system (UPS)(8,9). Proteins tagged with poly-ubiquitin chains are hydrolyzed into small peptides by the 26S proteasome in an energy-dependent manner. The 26S proteasome is assembled from a cylinder-shaped 20S proteolytic complex and a PA700 (19S) ATPase regulatory complex(10). The assembly and activity of the 26S proteasome is tightly regulated by a large number of cofactors and chaperones (8). Cancer cells are more exposed to proteotoxic stress due to high metabolic rates, reprogrammed energy metabolism and aneuploidy (5,11–13). Despite this pressure, they successfully proliferate and efficiently withstand this challenge by fully exploiting the cells' defense mechanisms against proteotoxic stress. For instance, constitutive activation of the heat shock factor protein 1 (HSF1)-regulated heat shock response (HSR) pathway is among the recurring features of malignant cells, and inhibition of molecular chaperones represents a promising therapeutic strategy for cancer treatment (14). In addition, increased proteasome activity can suppress aneuploidy-associated proteotoxic stress (12). Activation of proteasomal degradation by deletion of the proteasome-associated deubiquitylating enzyme UBP6 attenuates the aneuploidy-induced changes in cellular protein composition and improves cell fitness (15). The mechanisms by which cancer cells overcome proteotoxic stress are of considerable scientific and clinical interest as advances in this area may identify new therapeutic targets. Notably, proteasome inhibitors have anti-tumor activity and are clinically used for the treatment of multiple myeloma and mantle-cell lymphoma (16,17).

The rate-limiting step in proteolysis by the UPS is considered to be substrate ubiquitination. However, recent findings indicate that proteolysis rate is significantly changed by regulatory pathways that affect the activity of the 26S proteasome itself, for example by post-translational modifications of proteasome subunits, or by facilitating the assembly of the 26S proteasome from the core proteasome and the regulatory complexes (18,19). It has been previously shown that colon cancer cells increase expression of proteasome subunits in a concerted manner(20). However, up-regulating the levels of proteasome subunits, while important, is not sufficient to significantly increase proteasome activity. Indeed, the levels of functional 26S proteasomes depend not only on the expression of its subunits but also on their precise assembly. Work in yeast clearly demonstrates that assembly of 26S can vary significantly to meet the changing proteolytic needs of a cell(21).

Here we investigated a possible role of 26S proteasome assembly for protein homeostasis during tumorigenesis of the mouse gut epithelium. We show that 26S proteasome assembly is highly increased upon tumorigenic transformation of the gut epithelium. Importantly, this increase in 26S assembly is cell-autonomous and occurs exclusively in transformed cells, but not in other rapidly dividing cells. In addition, levels of the proteasome assembly inhibitor PSMD5/S5B are significantly decreased in tumors, and re-expression of PSMD5 blocks 26S proteasome assembly. Collectively, these results suggest that intestinal cancer cells escape proteotoxic stress by reducing PSMD5 to stimulate 26S proteasome assembly.

Methods

Mice

APC$^{min/+}$ mice were purchased from JAX® Mice. We induced colonic tumors using the AOM-DSS protocol as previously described(22). Briefly, we injected AOM (10mg/kg body weight) into 8–10 week old mice. 6 days after injection we treated mice with 2% DSS solution for 5 days. We repeated the DSS treatment on days 26–31 and on days 46–51. We assessed tumors 6–8 months after AOM injection. All experiments involving mice were approved by IACUC of The Rockefeller University (protocol number 14703-H).

Organoids

Intestinal crypts or tumors from WT, APC$^{min/+}$ and AOM-DSS treated mice were isolated as previously described (23,24), with several modifications: large bowels with and without tumors were flushed with cold PBS and opened longitudinally, washed with 70% ethanol. Large bowel tumors were dissected from normal large bowel. Normal large bowels and tumors were agitated in a solution of 2 mM EDTA in PBS for 30 minutes at 4°C. Tumors were dissociated using 70μm strainer.

Crypts were collected as described and embedded onto Matrigel (BD Biosciences) with 50 μl/well in 24-well plates. DMEM/F12 culture medium (Gibco), containing Glutamax (Gibco) and Penicillin/Streptomycin was supplemented with B27 (Gibco, 1:50), 100 ng/ml murine Noggin (Peprotech), 20 ng/ml murine EGF (Peprotech), 10 ng/ml human basic-FGF (Peprotech) and 250 ng/ml human R-Spondin1 (Peprotech), 100ng/ml mouse Wnt-3a (Peprotech) and 10mM Nicotinamide (Sigma) for large bowel organoids. Tumor organoids were cultured in medium containing only B27 (Gibco, 1:50), 100 ng/ml murine Noggin (Peprotech) and 20 ng/ml murine EGF (Peprotech) supplements.

Lentiviral infection was used to transduce genes into advanced tumor organoids. We generated recombinant lentiviral particles expressing mouse PSMD5 in HEK293T. Because lentivirus particles cannot penetrate the Matrigel layer, we incubated dissociated organoids with viral particles in liquid media for 6 hours 37°C under 5% CO_2 (v/v). Next, cells were embedded in Matrigel and grown into organoids. 2–3 days after plaiting of cells puromycin was added (5μg/ml) to the medium for selection of successfully transduced cells.

Protein translation rate (SUnSET)

The rate of protein translation was measured using the non-radioactive SUnSET labeling method(25). Briefly, Puromycin (4 μM) was added to culture medium of organoids for 30 minutes, then organiods were harvested and Puromycin incorporation was detected by Western blot using an anti-Puromycin antibody, clone 12D10 (1:5,000, Sigma). To label new synthesized proteins *in-vivo,* we injected into peritoneum (IP)Puromycin (0.04 μM/gr of body weight of mice). We euthanized animals 30 min after Puromycin injection and analyzed tissues by Western blot using an anti-Puromycin antibody, clone 12D10 (1:5,000, Sigma).

Cell Culture and DNA Transfection

HEK293T and HT-29 cells (purchased from ATCC) were grown in DMEM containing 10% fetal bovine serum and penicillin/streptomycin at 37°C under 5% CO_2 (v/v). For lentiviral production HEK293T were transfected with the appropriate vectors using X-tremeGENE 9 DNA Transfection Reagent (Roche) according to the manufacturer's instructions.

Native gel electrophoresis

Protein extracts of tissues were prepared in buffer (50 mM Tris-HCl (pH 8.0), 5 mM $MgCl_2$, 0.5 mM EDTA, 2 mM ATP, 0.2% NP4, protease inhibitor, phosphatase inhibitor (Pfizer)), using glass dounce or polytron homogenizers. Extracts were clarified by centrifugation at 14, 000 RPM for 30 min to remove nuclei and cell debris, and protein concentrations were measured by Bradford assay. To resolve proteasomes, 26-well 3–8% Tri-acetate gels (Criterion) were used. Samples were mixed with 2X native loading buffer (Bio-Rad) just before loading. Electrophoresis were carried out at RT (1 hour at 50V) and then at 4°C for an additional 5 hours at 120V, in running buffer (0.45M Tris, 0.45M Boric Acid, 5mM EDTA, 12.5 mM $MgCl_2$, supplemented with 0.5 mM DTT, 0.5 mM ATP). For immunoblotting, proteins in native gels were transferred to PVDF membranes. 26S and 20S proteasomes were detected with anti-RPT1 (19S specific) and anti-Alpha7 (20S specific) antibodies (Enzo). Purified bovine 20S, and 26S proteasomes (UBPBio), were used as standards.

Antibodies and Western blot

Protein extracts were prepared as for Native gel electrophoresis. For western blotting, proteins were resolved by SDS-PAGE and transferred onto a 0.45 μm PVDF membrane. Membranes were blocked overnight at 4°C with 5% milk in phosphate buffered saline (PBS) and 0.5% Tween-20 (PBST). Membranes were incubated for 60 min with one of the following antibodies: Polyubiquitin-FK2 (Enzo,1:2000), Actin HRP conjugated (Cell Signaling,1:10000), p-S6 (Cell signaling, 1:1000), PSMD 5 (TermoFisher, 1:4000), ECM 29 (Abcam, 1:1000), PSMD 11 (Cell Signaling, 1:4000), RPT1 (Enzo, 1:1000), RPT3 (Enzo, 1:1000), Alpha2 (Enzo, 1:1000), Alpha4 (Enzo, 1:1000), Alpha7 (Enzo, 1:1000), Tubulin (Sigma, 1:1000). Primary antibodies were detected by secondary species-specific HRP-congugated antibodies (Jackson ImmunoResearch, 1:5000). Detection was performed with Amersham ECL Western Blotting Detection Reagent (GE Healthcare).

ImageJ software was used for densitometric quantitation. Protein bands were selected with rectangle tool, picks were isolated and area of the pick was calculated. Background calculation was done using same rectangle placed just below protein bands. Background pick values were subtracted form corresponding protein band picks values.

Proteasome activity assay

Proteasome activity was measured using Proteasome-Glo (Promega), which detects chymotrypsin-like activity in cell-based assays. For proteasome activity assays, tissue/cell lysates were prepared in PIPES buffer (50 mM PIPES, 1 mM $MgCl_2$, 50 mM NaCl, 2 mM EGTA, and 2 mM ATP) using glass dounce. 50 μg of protein extracts were aliquoted in duplicates to a black 96-well plate. Samples were assayed for proteasome activity with the

Proteasome-Glo Chymotrypsin-like Cell-Based Assay (Promega) in a Spectramax M2 reader (Molecular Devices).

For PSMD5 KD experiments - HT-29 (5×10^3 cells per well) were seeded in a white 96 well plate. 24 hours later cells were transfected with control or PSMD5 siRNA (Dharmacon OnTarget pull of 5 different targeting RNAi's) using Dharmafect1 transfection reagent as recommended by the manufacturer. Cells were analyzed 5–6 days post transfection using Proteasome-Glo assay (Promega). Luciferase values were normalized to cell viability as measured by PrestoBlue (Thermo Fisher Scientific) in a parallel plate. Samples were analyzed in a Spectramax M2 reader (Molecular Devices).

Size-Exclusion Chromatography

Normal gut epithelium and tumors of $APC^{min/+}$ mice were lysed in 300 μL of buffer (50 mM Tris, pH 7.5, 150 mM NaCl, 10% glycerol, 5 mM $MgCl_2$, 0.22 μm-filtered and supplemented with 0.5% NP-40, 1 mM DTT, 1mM ATP, phosphatase inhibitor (Roche)) using glass dounce. Cell lysates were cleared twice by centrifugation, 0.22 μm-filtered, and quantified by Bradford protein assay. Equal amounts of each lysate (1.0 mg in 500 μL) were sequentially injected into a Superose 6 10/300 GL column (GE Healthcare) controlled by the ÄKTA-FPLC™ system (GE Healthcare). The column was pre-equilibrated and run with the above buffer without NP-40 at a rate of 0.2 mL/min. Fractions (0.25 mL each) were collected and 15 μL from each fraction was used in western blot analysis.

In-gel peptidase activity assay

Protein extracts of tissues were prepared and resolved on native gel as described above. For the in-gel peptidase activity assat, we carefully dislodged the resolving gel from the glass plate into a tray with buffer (50 mM Tris, pH 7.5, 150 mM NaCl, 5 mM $MgCl_2$, 5 mM ATP, 200 uM of suc-LLVY-AMC substrate (Bachem) with or without 0.02% SDS) and incubated it at 30 °C for 30 minutes in a shaker with slow agitation (~30 rpm). After that the gel was transferred from the tray to a UV trans-illuminator for analysis.

RNA-seq

Bulk population samples were processed by extracting RNA with RNeasy Plus Micro Kit (Qiagen) per the manufacturer's recommendations, and then 10ng of RNA from each sample was used to prepare RNAseq libraries using a modified SMART-Seq2 protocol as previously reported(26). The libraries were sequenced on an Illumina NextSeq 500. Due to different complexities between the early and advanced tumor organoid RNAseq libraries, the data was quantile normalized using the between Lane Normalization function of the EDASeq package in R. We then performed differential expression analysis on two biological repeats using the R package DESeq2(27), which fits a negative binomial generalized linear model (GLM).

Results

Protein translation is increased in intestinal tumors

The rate of protein translation is higher in tumors than normal tissue, although to date the exact timing of this switch has not been determined (28). First we directly measured protein

translation in two different mouse models of colon cancer, $APC^{min/+}$ and Azoxymethane/ Dextran sulfate sodium (AOM-DSS) treatment, with the non-radioactive SUface SEnsing of Translation (SUnSET) method (19). In the SUnSET method the antibiotic puromycin, a structural analog of aminoacyl tRNAs, is incorporated into the nascent polypeptide chain and prevents further elongation(25). We observed highly increased puromycin uptake in large bowel tumors of $APC^{min/+}$ mice compared to normal tissue 30 min after puromycin injection (Fig. 1A). Since puromycin prevents elongation, the resulting puromycin-tagged proteins are prematurely truncated, resulting in damaged proteins. The level of poly-ubiquitination(Poly-Ubi) in tumors and normal tissue was compared in order to determine if the increase in the amount of damaged proteins corresponds to increased stimulation of the ubiquitin-proteasome system. Indeed, as expected, a significant increase of poly-Ubi staining in tumors 30 min after puromycin injection was observed in large bowel tumors of $APC^{min/+}$ mice compared to normal tissue (Fig. 1B). In order to establish whether the observed increase in translation derives from transformed epithelial cells or other cells residing in tumors, we generated organoids from normal large bowel epithelium and from tumors of DSS-AOM mice. Tumor organoids had significantly higher puromycin uptake than normal tissue organoids (Fig. 1C). Taken together, these results show that protein translation is rapidly increased upon transformation of the intestinal epithelium.

Increased proteasome assembly in intestinal tumors of $APC^{min/+}$ and AOM-DSS mice

Next, we investigated whether increased protein synthesis in intestinal tumors is counterbalanced by increased protein degradation. The results shown in Figure 1B demonstrate that the first step of UPS-mediated protein degradation, the conjugation of substrates with ubiquitin, occurs efficiently. In order to assess effects on the 26S proteasome, we first assayed levels of several individual proteasome subunits (Fig. 2A). We did not detect substantial differences in the levels of proteasome subunits between normal tissue and tumors (Fig. 2A). In order to assess the capability of the proteasome to degrade poly-ubiquitinated proteins, we measured total proteasome proteolytic activity using a Proteasome-Glo™ Assay (Promega) on cell lysates from large and small bowel tumors and the corresponding normal gut epthelium of $APC^{min/+}$ mice. Tumors from the small and large bowel of $APC^{min/+}$ mice displayed 3 times higher proteasomal activity compared to corresponding normal tissues (Fig. 2B). Subsequently, we used native gel and size exclusion chromatography to compare the proteasome content of normal gut epithelium and tumors. In order to detect all proteasomal sub-complexes we used native gel electrophoresis followed by in-gel suc-LLVY-AMC activity assay with Sodium dodecyl sulfate (SDS). Treatment with SDS allows detection of 20S proteasomes activity, which is otherwise not detected due to the closed gate of the 20S proteasome. We found that large bowel tumors of AOM-DSS mice had higher levels of 26S proteasomes and lower levels of 20S compared to normal tissue, indicating enhanced assembly of 26S in tumors (Fig. 2C). Next, we evaluated 26S proteasome assembly in large bowel epithelium and tumors of $APC^{min/+}$ mice using native gel electrophoresis (Fid. 2D). We quantitated Western blots from three independent experiments and present data as 26S/20S ratio. Again, this revealed a significant shift in the 20S/26S ratio to a higher portion of 26S proteasomes in tumors. Since 26S proteasomes are the active particles responsible for degradation of poly-ubiquitinated proteins, these findings indicate that tumors have increased proteolytic potential. In order to further confirm these

findings, we analyzed endogenous proteasome complexes from small bowel tumors and normal tissues of $APC^{min/+}$ mice using size exclusion chromatography. These experiments revealed a considerable shift towards larger proteasomal complexes without affecting the total amount of 19S complexes in tumors, as evaluated with an anti-RPT1 antibody (Fig. 2E). We also performed quantitative analyses and calculated the total amount of 26S (first peak) and 20S (second peak) proteasomes in tumors and normal tissue.(Fig. 2E table). This analysis revealed again a reduction of unassembled 20S and elevated levels of 26S particles in tumors, indicating enhanced 26S assembly (Fig. 2E). Collectively, these results show that malignant transformation of intestinal epithelial cells is associated with increased 26S proteasome assembly.

Increased proteasomal assembly is tumor specific

One of the most important histopathological features of intestinal neoplasia is tumor-associated inflammation. Inflammatory cells not only reside in the tumor but also play important pathophysiological roles in the development of a tumor by secreting various cytokines. Since inflammatory cells are rapidly dividing and share many metabolic features with neoplastic cells, we wanted to clarify their potential contribution to increased 26S assembly in tumors. For this purpose, we induced colitis in C57BL/6 mice using 2.5% DSS in drinking water for 7 days. Next, we determined the proteasome levels of large bowel epithelium and mesenteric lymph nodes of healthy and DSS-treated animals using native gel electrophoresis. We observed no change in proteasome assembly in the colonic tissue as a result of inflammation, and no differences between mesenteric lymph nodes and large bowel epithelium were observed irrespective of the inflammation (Fig. 3A). In contrast, 26S assembly was increased in large bowel tumors (Fig. 3A). In order to further validate that the change in 26S proteasome assembly is caused by transformation of epithelial cells themselves, and not from other cell types, we grew organoids from large bowel tumors and normal epithelium. Next, we performed native gel electrophoresis analysis of normal tissue and large bowel organoids and found an increase in the assembly of 26S proteasomes in tumor organoids compared to normal tissue (Fig. 3B).

26S assembly increases with tumor progression

Unlike humans, $APC^{min/+}$ mice do not live long enough to develop adenocarcinomas as they die due to bleeding from gut adenomas(29). Growing these tumors as organoids enabled us to study tumor progression *ex vivo*. After 20 passages large bowel tumor organoids started to change their shape and form less symmetric and organized spheres (Fig. 4A). We hypothesized that the change in the shape represents *ex vivo* progression of large bowel adenomas of $APC^{min/+}$ mice to carcinomas. In order to validate our hypothesis we subcutaneously injected 5×10^5 cells into NSG mice. 6 weeks later we detected subcutaneous tumors only in mice injected with the advanced organoids (Fig. 4B, Sup S1A). Histological examination of these tumors revealed cells with different nuclear size and shape, prominent nucleoli and almost no gland formation, resembling the histology of poorly differentiated human adenocarcinoma (Fig. 4C). Next, we measured protein synthesis in early and advanced tumor organoids and found a dramatic increase in protein synthesis in the advanced tumor organoids (Fig. 4D). Since we hypothesized that increased translation of advanced tumor organoids must be counterbalanced by enhanced degradation, we measured

selected individual proteasome subunits and the proteasomal sub-complex content of early and advanced tumor organoids using PAGE-SDS and native gel electrophoresis, respectively (Fig. S1B, Fig. 4E). Similarly to what we saw in tumors and normal epithelium, we did not observe substantial differences in the levels of individual subunits. However we detected an increase in 26S proteasomes in advanced tumor organoids compared to early tumor organoids (Fig. 4E). In order to validate that these 26S proteasomes are active, we performed in-gel suc-LLVY-AMC activity assays without SDS, which allows specific detection of active 26S proteasomes. Advanced tumor organoids contained more active single and double-capped 26S proteasomes (Fig. 4F upper blot) at the expense of free 20S proteasomes detected by anti-20S immunobloting (Fig. 4F lower blot). Recent studies showed that the Rapamycin complex 1 (mTORC1) is linked to the regulation of protein degradation by proteasomes (30,31). Therefore, we checked early and advanced organoids and found a strong activation of mTORC1 in advanced organoids as judged by the levels of pS6, which probably contributes to increased translation (Fig. 4G). In order to investigate whether the mTORC1 pathway is responsible for the enhanced assembly of 26S in the advanced organoids we treated these organoids with Rapamycin. Although Rapamycin treatment resulted in the suppression of the mTORC1 pathway, we did not detect a substantial decrease in the assembly of 26S since amounts of both 26S and 20S declined under these conditions (Fig 4G&4H), indicating that mTORC1 pathway, though activated, is not responsible for the enhanced 26S assembly in advanced tumor organoids.

PSMD-5 promotes tumor-associated proteasome assembly

In order to identify potential genes that can explain the difference in 26S assembly between early and advanced tumor organoids we performed RNA-seq analysis on the two lines of organoids. Using this strategy we identified 50 proteasome related genes, of which the expression of 17 changed more than two fold (Table 1 and S2A). Since we were interested in factors that may increase assembly of the 26S proteasome in the advanced organoids we looked for previously reported enhancers and inhibitors of assembly in the list of up- and down-regulated genes respectively. This revealed significantly decreased expression of one proteasome assembly inhibitor - PSMD5 and increased expression of two activators - ECM29 and PSMD11(32–34). Western blot analysis of early and advanced tumor organoids demonstrated significant reduction of PSMD5 and elevation of ECM29 in advanced organoids, with no change in PSMD11 (Fig. 5A). Subsequently we checked expression of these candidate proteins in the large bowel tumors compared to normal epithelium. Whilst no increase in the levels of ECM-29 and PSMD11 proteins was observed, there was a subtle reduction in the levels of PSMD5 in tumors compared to normal tissue (Fig. S2B, 2A, and 5B). Next, we plated xenografts originating from advanced tumor organoids and overexpressed PSMD5. Overexpression of PSMD5 caused a decrease in 26S levels and an increase in the amount of unassembled 20S, demonstrating reduced proteasome assembly as expressed in 26S/20S ratio (Fig. 5C). Additionally, PSMD5 overexpression resulted in the reduction of total proteasome activity (Fig. 5D). Moreover, the decrease in 26S proteasomes led to accumulation of poly-ubiquitinated proteins (Ub K48) (Fig. 5C). In order to check whether suppression of PSMD5 may boost proteasome assembly and activity in human colorectal cancer, we knocked down PSMD5 in a human colorectal cancer cell line, HT-29 (Fig. 5E). Indeed, down-regulation of PSMD5 led to enhanced assembly of 26S and

increased total proteasome activity similarly to what we found in the murine model (Fig. 5E and 5F).

These observations indicate that PSMD5 promotes 26S proteasome assembly during the malignant transformation of the intestinal epithelium and illustrate the importance of this mechanism for protein homeostasis in tumors.

Discussion

It is well accepted that proteostasis in cancer cells changes dramatically upon malignant transformation(5,11,12,14,35). In this study we utilized mouse models of colorectal cancer, $APC^{min/+}$ and DSS-AOM mice, to explore changes in proteostasis after malignant transformation. It is well-documented that protein translation is enhanced upon malignant transformation(14,28,36). We show that an increase in protein synthesis is an intrinsic feature of transformed cells since it occurs in organoids, outside the cellular context of the organism. Using a new model of *ex vivo* tumor progression from adenoma to carcinoma we demonstrate that global protein synthesis further increases with tumor progression. These changes in protein synthesis of mouse colon cancer cells make organoids an attractive model to study adaptation responses of transformed cells to the proteotoxic stress.

Multiple mechanisms have been suggested to protect cancer cells from proteotoxic stress. The UPS is one of the two main protein degradation machineries and we show here that poly-ubiquitination of damaged proteins is very efficient in bowel tumors of mice (Fig. 1B). This increase in poly-ubiquitination is accompanied by increased proteasome activity. One means of proteasome activation in cancer is a global increase in the expression of genes encoding proteasome subunits. It was suggested that mTORC1 increases the amounts of proteasome subunits through induction of the transcription factor nuclear factor erythroid-derived 2-related factor 1 (NRF1)(1), although this result remains controversial(30). In our model Rapamycin treatment resulted in the reduction of the levels of 26S but not in the assembly of 26S. Another study showed an elevation in the number of proteasomal subunits through induction of nuclear factor E2-related factor 2 (Nrf2)(20). While up-regulation of individual protesomal subunits is important to increase the amount of active 26S proteasomes, it is likely that additional mechanisms contribute to assure proper assembly of these individual subunits into active 26S proteasomes. Moreover, it was shown that there is no change in the levels of 18 individual proteasome subunits upon acute loss of APC despite an increase in translation (37). In this study, we show that assembly of 26S from 20S and 19S is increased in the intestinal tumors. This increase in assembly 26S is not solely due to up-regulation of individual subunits as we saw a concomitant decrease in the amounts of 20S sub-complexes. Moreover, we show that the increase in assembly occurs only in transformed cells and not in other rapidly dividing cells, such as inflammatory cells. We also observed increased 26S proteasome assembly in intestinal tumors growing *ex vivo* as organoids, indicating that it is a cell autonomous response independent of the *in vivo* tumor microenvironment. Finally, we found that 26S assembly increases with tumor progression. Collectively, these results suggest that 26S proteasome assembly increases as tumors progress to counter-balance elevated proteotoxic stress that under these conditions.

In order to gain insight into the molecular mechanism underlying the increased 26S proteasome assembly in intestinal tumors, we performed RNA-seq analysis of early and advanced tumor organoids. This analysis did not reveal a global change in the expression of genes encoding proteasome subunits. On the other hand, we identified two genes, ECM-29 and PSMD5, as possible regulators of 26S assembly based on clear changes of their expression in advanced organoids. Expression of ECM-29, a well-known enhancer of 26S assembly, was significantly increased in advanced organoids but not in the large bowel tumors. Interestingly, it has been suggested that ECM-29 is an oncogene in castration-resistant prostate cancer(33). Our data are consistent with an oncogenic function of ECM-29 in advanced intestinal tumors but a clear demonstration will require further functional studies. Here we focused on PSMD5, which had significantly reduced expression of both mRNA and protein in advanced tumors. PSMD5/S5b is a chaperone that promotes assembly of the base sub-complex of the 19S proteasomes and has complex and seemingly opposing roles for proteasome assembly and activity. One the one hand, PSMD5 is important for the formation of the PSMD5-Rpt1-Rpt2-Rpn1 complex during 19S assembly (38,39). Hsm3, the yeast ortholog of PSMD5, can associate with 19S sub-complexes via a carboxy-terminal domain of the Rpt1 base subunit, and Hsm3Δ cells display defects in 19S base assembly (40). The crystal structure of yeast Hsm3 suggests that Hsm3 also binds to Rpt2 and serves as a scaffold protein for Rpt1-Rpt2-Rpn1 complex assembly (41). On the other hand, in *Drosophila* and mammalian elevated PSMD5 can inhibit 26S proteasome assembly and activity (19,32). It was also shown that interaction between PSMD5 and Rpt1 is essential for proteasome inhibition(32). Moreover, amino acids 180–188 of PSMD5 are indispensable for 26S proteasome inhibition, and a specific point mutation (R184E) can abolish this inhibitory effect (32). It is important to note that the association of PSMD5with 19S sub-complex proteins is transient, and removal of this chaperone promotes 26S proteasome assembly ((19,32)). Therefore, it appears that PSMD5/S5b levels need to be very carefully regulated, and perturbations may have different effects depending on context. Here we show that PSMD5 is down-regulated in intestinal tumors. Moreover, as the tumor progresses PSMD5 is silenced at the transcriptional level and this is allows for increased assembly of 26S proteasomes. Consistent with this model, we found that over-expression of PSMD5 in advanced intestinal tumor organoids reduced total proteasome activity, 26S proteasome levels and caused the accumulation of poly-ubiquitinated proteins. Additionally, suppression of PSMD5 in a human colorectal cell line boosts 26S proteasome assembly and total proteasome activity. Therefore, it appears that one of the mechanisms intestinal tumor cells utilize to maintain protein homeostasis in the face of increased protein synthesis is silencing of PSMD5 expression to stimulate 26S proteasome assembly (Fig. 5G). Interestingly, a recent study identified PSMD5 as the most frequently transcriptionally suppressed 19S proteasome subunit in a dataset of thousands of human cancer cell lines(42). This work indicates that PSMD5 transcriptional suppression is an epigenetic process regulated by DNA promoter methylation. Moreover, PSMD5 suppression was found to be associated with resistance to Bortezomib, which could be explained by our finding of enhanced 26S assembly. However, in contrast to this study we did not observe a general suppression of 19S, but rather found five different 19S subunits to be up-regulated in advanced tumor organoids. We envision that this mechanism assures that proteasomes are not rate-limiting for protein breakdown in the context of increased metabolic rates of tumor cells. Proteasome

inhibitors are clinically used for the treatment of multiple myeloma and mantle cell lymphoma(16). However, proteasome inhibitors have multiple side effects as they are non-selective agents that impair protein breakdown in both malignant and normal cells. We propose that targeting proteasomal assembly in cancer cells may be more selective and have less side effects toxicity. Therefore, targeting cancer-associated proteasome assembly pathways may provide new opportunities for cancer therapy.

Supplementary Material

Refer to Web version on PubMed Central for supplementary material.

Acknowledgments

Financial support: Iris and Jumming Le Foundation and The Rockefeller University Center for Clinical and Translational Science to A. Levin, NCATS grant UL1 TR000043 to A. Levin, a gift from the Leona M. and Harry B. Helmsley Charitable Trust to A. Levin, and NIH grant RO1GM60124 to H. Steller.

We thank Sigi Benjamin and other members of our lab for valuable discussions, and Sohail Tavazoi for feedback on the manuscript. This work was supported by the Iris and Jumming Le Foundation and The Rockefeller University Center for Clinical and Translational Science, NCATS grant UL1 TR000043, a gift from the Leona M. and Harry B. Helmsley Charitable Trust, and NIH grant RO1GM60124 to H.S.

References

1. Zhang Y, Nicholatos J, Dreier JR, Ricoult SJ, Widenmaier SB, Hotamisligil GS, et al. Coordinated regulation of protein synthesis and degradation by mTORC1. Nature. 2014; 513(7518):440–3. DOI: 10.1038/nature13492 [PubMed: 25043031]
2. Suraweera A, Munch C, Hanssum A, Bertolotti A. Failure of amino acid homeostasis causes cell death following proteasome inhibition. Molecular cell. 2012; 48(2):242–53. DOI: 10.1016/j.molcel.2012.08.003 [PubMed: 22959274]
3. Fonseca R, Vabulas RM, Hartl FU, Bonhoeffer T, Nagerl UV. A balance of protein synthesis and proteasome-dependent degradation determines the maintenance of LTP. Neuron. 2006; 52(2):239–45. DOI: 10.1016/j.neuron.2006.08.015 [PubMed: 17046687]
4. Walter P, Ron D. The unfolded protein response: from stress pathway to homeostatic regulation. Science. 2011; 334(6059):1081–6. DOI: 10.1126/science.1209038 [PubMed: 22116877]
5. Luo J, Solimini NL, Elledge SJ. Principles of cancer therapy: oncogene and non-oncogene addiction. Cell. 2009; 136(5):823–37. DOI: 10.1016/j.cell.2009.02.024 [PubMed: 19269363]
6. Hershko A, Ciechanover A. The ubiquitin system. Annual review of biochemistry. 1998; 67:425–79. DOI: 10.1146/annurev.biochem.67.1.425
7. Glickman MH, Ciechanover A. The ubiquitin-proteasome proteolytic pathway: destruction for the sake of construction. Physiological reviews. 2002; 82(2):373–428. DOI: 10.1152/physrev.00027.2001 [PubMed: 11917093]
8. Collins GA, Goldberg AL. The Logic of the 26S Proteasome. Cell. 2017; 169(5):792–806. DOI: 10.1016/j.cell.2017.04.023 [PubMed: 28525752]
9. Livneh I, Cohen-Kaplan V, Cohen-Rosenzweig C, Avni N, Ciechanover A. The life cycle of the 26S proteasome: from birth, through regulation and function, and onto its death. Cell research. 2016; 26(8):869–85. DOI: 10.1038/cr.2016.86 [PubMed: 27444871]
10. Budenholzer L, Cheng CL, Li Y, Hochstrasser M. Proteasome Structure and Assembly. Journal of molecular biology. 2017; doi: 10.1016/j.jmb.2017.05.027
11. Dai C, Dai S, Cao J. Proteotoxic stress of cancer: implication of the heat-shock response in oncogenesis. J Cell Physiol. 2012; 227(8):2982–7. DOI: 10.1002/jcp.24017 [PubMed: 22105155]
12. Oromendia AB, Amon A. Aneuploidy: implications for protein homeostasis and disease. Disease models & mechanisms. 2014; 7(1):15–20. DOI: 10.1242/dmm.013391 [PubMed: 24396150]

13. Deshaies RJ. Proteotoxic crisis, the ubiquitin-proteasome system, and cancer therapy. BMC Biol. 2014; 12:94.doi: 10.1186/s12915-014-0094-0 [PubMed: 25385277]
14. Santagata S, Mendillo ML, Tang YC, Subramanian A, Perley CC, Roche SP, et al. Tight coordination of protein translation and HSF1 activation supports the anabolic malignant state. Science. 2013; 341(6143):1238303.doi: 10.1126/science.1238303 [PubMed: 23869022]
15. Santaguida S, Amon A. Short- and long-term effects of chromosome mis-segregation and aneuploidy. Nature reviews Molecular cell biology. 2015; 16(8):473–85. DOI: 10.1038/nrm4025 [PubMed: 26204159]
16. Manasanch EE, Orlowski RZ. Proteasome inhibitors in cancer therapy. Nature reviews Clinical oncology. 2017; 14(7):417–33. DOI: 10.1038/nrclinonc.2016.206
17. Crawford LJ, Irvine AE. Targeting the ubiquitin proteasome system in haematological malignancies. Blood reviews. 2013; 27(6):297–304. DOI: 10.1016/j.blre.2013.10.002 [PubMed: 24183816]
18. Lokireddy S, Kukushkin NV, Goldberg AL. cAMP-induced phosphorylation of 26S proteasomes on Rpn6/PSMD11 enhances their activity and the degradation of misfolded proteins. Proceedings of the National Academy of Sciences of the United States of America. 2015; 112(52):E7176–85. DOI: 10.1073/pnas.1522332112 [PubMed: 26669444]
19. Cho-Park PF, Steller H. Proteasome regulation by ADP-ribosylation. Cell. 2013; 153(3):614–27. DOI: 10.1016/j.cell.2013.03.040 [PubMed: 23622245]
20. Arlt A, Bauer I, Schafmayer C, Tepel J, Muerkoster SS, Brosch M, et al. Increased proteasome subunit protein expression and proteasome activity in colon cancer relate to an enhanced activation of nuclear factor E2-related factor 2 (Nrf2). Oncogene. 2009; 28(45):3983–96. DOI: 10.1038/onc.2009.264 [PubMed: 19734940]
21. Hanssum A, Zhong Z, Rousseau A, Krzyzosiak A, Sigurdardottir A, Bertolotti A. An inducible chaperone adapts proteasome assembly to stress. Molecular cell. 2014; 55(4):566–77. DOI: 10.1016/j.molcel.2014.06.017 [PubMed: 25042801]
22. Neufert C, Becker C, Neurath MF. An inducible mouse model of colon carcinogenesis for the analysis of sporadic and inflammation-driven tumor progression. Nature protocols. 2007; 2(8):1998–2004. DOI: 10.1038/nprot.2007.279 [PubMed: 17703211]
23. Sato T, Vries RG, Snippert HJ, van de Wetering M, Barker N, Stange DE, et al. Single Lgr5 stem cells build crypt-villus structures in vitro without a mesenchymal niche. Nature. 2009; 459(7244):262–5. DOI: 10.1038/nature07935 [PubMed: 19329995]
24. Sato T, Stange DE, Ferrante M, Vries RG, Van Es JH, Van den Brink S, et al. Long-term expansion of epithelial organoids from human colon, adenoma, adenocarcinoma, and Barrett's epithelium. Gastroenterology. 2011; 141(5):1762–72. DOI: 10.1053/j.gastro.2011.07.050 [PubMed: 21889923]
25. Schmidt EK, Clavarino G, Ceppi M, Pierre P. SUnSET, a nonradioactive method to monitor protein synthesis. Nature methods. 2009; 6(4):275–7. DOI: 10.1038/nmeth.1314 [PubMed: 19305406]
26. Picelli S, Faridani OR, Bjorklund AK, Winberg G, Sagasser S, Sandberg R. Full-length RNA-seq from single cells using Smart-seq2. Nature protocols. 2014; 9(1):171–81. DOI: 10.1038/nprot.2014.006 [PubMed: 24385147]
27. Love MI, Huber W, Anders S. Moderated estimation of fold change and dispersion for RNA-seq data with DESeq2. Genome biology. 2014; 15(12):550.doi: 10.1186/s13059-014-0550-8 [PubMed: 25516281]
28. Barna M, Pusic A, Zollo O, Costa M, Kondrashov N, Rego E, et al. Suppression of Myc oncogenic activity by ribosomal protein haploinsufficiency. Nature. 2008; 456(7224):971–5. DOI: 10.1038/nature07449 [PubMed: 19011615]
29. Moser AR, Pitot HC, Dove WF. A dominant mutation that predisposes to multiple intestinal neoplasia in the mouse. Science. 1990; 247(4940):322–4. [PubMed: 2296722]
30. Zhao J, Zhai B, Gygi SP, Goldberg AL. mTOR inhibition activates overall protein degradation by the ubiquitin proteasome system as well as by autophagy. Proceedings of the National Academy of Sciences of the United States of America. 2015; 112(52):15790–7. DOI: 10.1073/pnas.1521919112 [PubMed: 26669439]

31. Zhao J, Goldberg AL. Coordinate regulation of autophagy and the ubiquitin proteasome system by MTOR. Autophagy. 2016; 12(10):1967–70. DOI: 10.1080/15548627.2016.1205770 [PubMed: 27459110]
32. Shim SM, Lee WJ, Kim Y, Chang JW, Song S, Jung YK. Role of S5b/PSMD5 in proteasome inhibition caused by TNF-alpha/NFkappaB in higher eukaryotes. Cell reports. 2012; 2(3):603–15. DOI: 10.1016/j.celrep.2012.07.013 [PubMed: 22921402]
33. Goto Y, Kojima S, Nishikawa R, Kurozumi A, Kato M, Enokida H, et al. MicroRNA expression signature of castration-resistant prostate cancer: the microRNA-221/222 cluster functions as a tumour suppressor and disease progression marker. British journal of cancer. 2015; 113(7):1055–65. DOI: 10.1038/bjc.2015.300 [PubMed: 26325107]
34. Vilchez D, Boyer L, Morantte I, Lutz M, Merkwirth C, Joyce D, et al. Increased proteasome activity in human embryonic stem cells is regulated by PSMD11. Nature. 2012; 489(7415):304–8. DOI: 10.1038/nature11468 [PubMed: 22972301]
35. Anderson DJ, Le Moigne R, Djakovic S, Kumar B, Rice J, Wong S, et al. Targeting the AAA ATPase p97 as an Approach to Treat Cancer through Disruption of Protein Homeostasis. Cancer cell. 2015; 28(5):653–65. DOI: 10.1016/j.ccell.2015.10.002 [PubMed: 26555175]
36. White RJ. RNA polymerases I and III, growth control and cancer. Nature reviews Molecular cell biology. 2005; 6(1):69–78. DOI: 10.1038/nrm1551 [PubMed: 15688068]
37. Hammoudi A, Song F, Reed KR, Jenkins RE, Meniel VS, Watson AJ, et al. Proteomic profiling of a mouse model of acute intestinal Apc deletion leads to identification of potential novel biomarkers of human colorectal cancer (CRC). Biochemical and biophysical research communications. 2013; 440(3):364–70. DOI: 10.1016/j.bbrc.2013.08.076 [PubMed: 23998936]
38. Le Tallec B, Barrault MB, Guerois R, Carre T, Peyroche A. Hsm3/S5b participates in the assembly pathway of the 19S regulatory particle of the proteasome. Molecular cell. 2009; 33(3):389–99. DOI: 10.1016/j.molcel.2009.01.010 [PubMed: 19217412]
39. Kaneko T, Hamazaki J, Iemura S, Sasaki K, Furuyama K, Natsume T, et al. Assembly pathway of the Mammalian proteasome base subcomplex is mediated by multiple specific chaperones. Cell. 2009; 137(5):914–25. DOI: 10.1016/j.cell.2009.05.008 [PubMed: 19490896]
40. Funakoshi M, Tomko RJ Jr, Kobayashi H, Hochstrasser M. Multiple assembly chaperones govern biogenesis of the proteasome regulatory particle base. Cell. 2009; 137(5):887–99. DOI: 10.1016/j.cell.2009.04.061 [PubMed: 19446322]
41. Barrault MB, Richet N, Godard C, Murciano B, Le Tallec B, Rousseau E, et al. Dual functions of the Hsm3 protein in chaperoning and scaffolding regulatory particle subunits during the proteasome assembly. Proceedings of the National Academy of Sciences of the United States of America. 2012; 109(17):E1001–10. DOI: 10.1073/pnas.1116538109 [PubMed: 22460800]
42. Tsvetkov P, Sokol E, Jin D, Brune Z, Thiru P, Ghandi M, et al. Suppression of 19S proteasome subunits marks emergence of an altered cell state in diverse cancers. Proceedings of the National Academy of Sciences of the United States of America. 2017; 114(2):382–7. DOI: 10.1073/pnas.1619067114 [PubMed: 28028240]

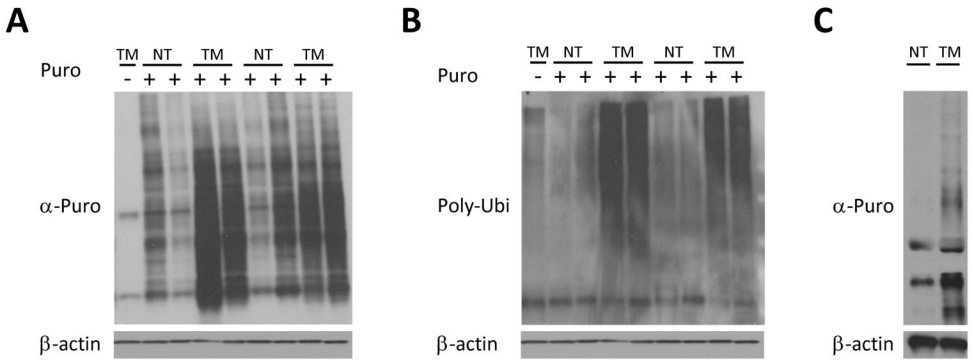

Figure 1. Protein translation is significantly increased in intestinal tumors

A. Anti-puromycin western blot of large bowel normal tissue (**NT**) and tumorous tissue (**TM**) of 6 month old $APC^{min/+}$ mice and their sibling controls (8 mice: lanes 2–5 are females and 6–9 are males), 30 minutes after injection with 0.04 uMol/gr of Puromycin, showing significantly greater puromycin uptake in large bowel tumors of $APC^{min/+}$ mice compared to normal tissue. **B.** anti-Polyubiquinated (FK-2) western blot of the samples from **A**., showing dramatic increase in the polyubiquitinated proteins in tumors. **C.** Anti-puromycin western blot of large bowel normal tissue and tumor organoids from AOM-DSS mice **(NT** and **TM respectively**). Organoids were cultured in the presence of 4 uM Puromycin for 30 min, showing significantly higher puromycin uptake in tumor organoids.

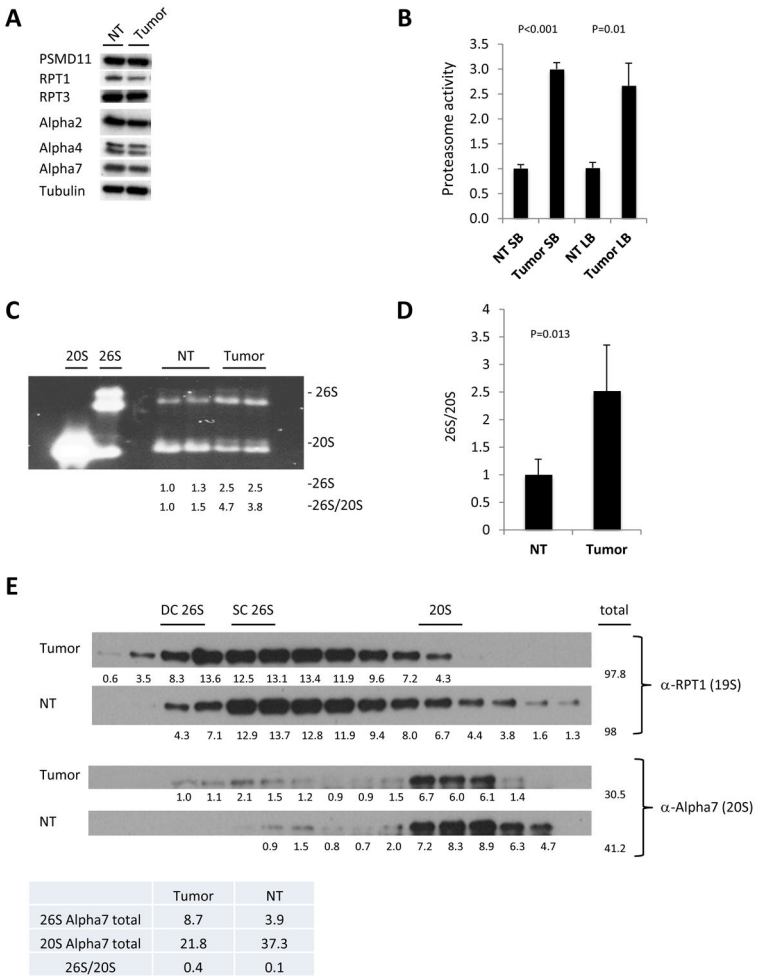

	Tumor	NT
26S Alpha7 total	8.7	3.9
20S Alpha7 total	21.8	37.3
26S/20S	0.4	0.1

Figure 2. Enhanced 26S proteasome assembly in murine gut tumors

A. Western blot of large bowel normal tissue and tumors from APC$^{min/+}$ mice of several individual proteasome subunits. **B.** Proteasome activity in normal tissue (NT) and tumors isolated from the small bowel (SB) and large bowel (LB). Values obtained for normal tissue were set as 1. The error bars represent the standard deviation from 2 biological samples per group measured in duplicates. The significance (p) between NT and tumor activity is shown. Statistical analysis was performed with a two-tailed paired *t*-test. **C.** In gel suc-LLVY-AMC activity with 0.02% SDS measured in large bowel tumors and normal tissue (NT) of AOM-DSS mice, demonstrating higher levels of 26S proteasomes and lower levels of 20S compared in tumors, indicating enhanced assembly of 26S in tumors. Densitometry was performed using ImgeJ. 26S proteasome assembly status(26S/20S) is reported as the intensity of 26S divided by intensity of 20S. D. Pooled densitometric quantitation of native gels of APC$^{min/+}$ mice normal tissue and tumors from three independent experiments, 26S proteasome assembly status (26S/20S) is reported as the intensity of 26S divided by intensity of 20S. The error bars represent the standard deviation from measurements of 4 biological samples. Statistical analysis was performed with a *t*-test. E. Western blot analysis of fractions from size exclusion chromotography of tumor and normal tissue (NT). Blotting with α-RPT1 antibody shows shift towards larger proteasomal complexes in the tumors

while blotting with α-Alpha7 antibody reveals more doubly and singly capped proteasomes species at the expense of unassembled 20S in the tumors. DC 26S – Double capped 26S, SC 26S – Single capped 26S. Densitometry was performed using ImgeJ. Table below the blots shows total of 26S and 20S peaks detected with anti-Alpha7 antibody.

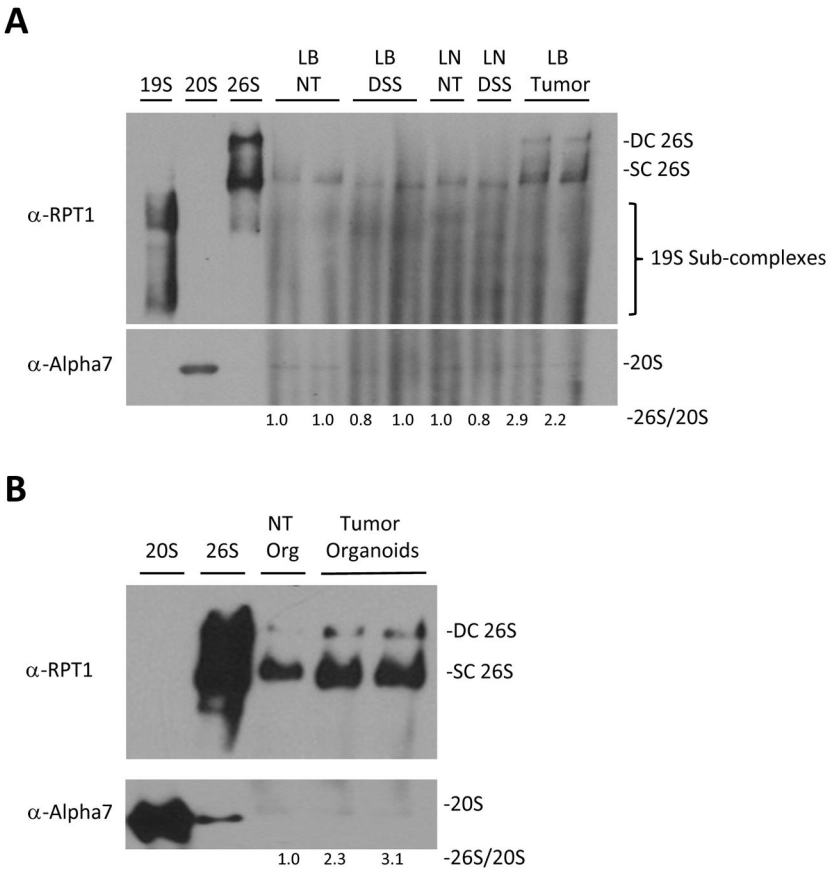

Figure 3. Enhanced assembly of 26S proteasomes, exclusively in the tumors and not other rapidly dividing cells

A. Western blot analysis following native gel electrophoresis of large bowel tumors of $APC^{min/+}$ mice (LB Tumor), large bowel epithelium of their littermate controls (LB NT), large intestinal epithelium of DSS induced colitis mice (LB DSS) and mesenteric lymph nodes of WT (LN) and DSS treated mice (LN DSS). It demonstrates high level of 26S proteasomes exclusively in the tumors irrespectively of inflammation. **B.** Western blot analysis following native gel electrophoresis of organoids from large bowel normal tissue and tumors of $APC^{min/+}$ mice shows increase in the assembly of 26S protesomes in tumor organoids compared to normal tissue. **26S and 20S** were detected by anti-RPT1 and anti-Alpha7 antibodies respectively. **DC 26S** – Double capped 26S, **SC 26S** – Single capped 26S. Densitometry was performed using ImgeJ. 26S proteasome assembly status(26S/20S) is reported as the intensity of 26S (DC+SC) divided by intensity of 20S.

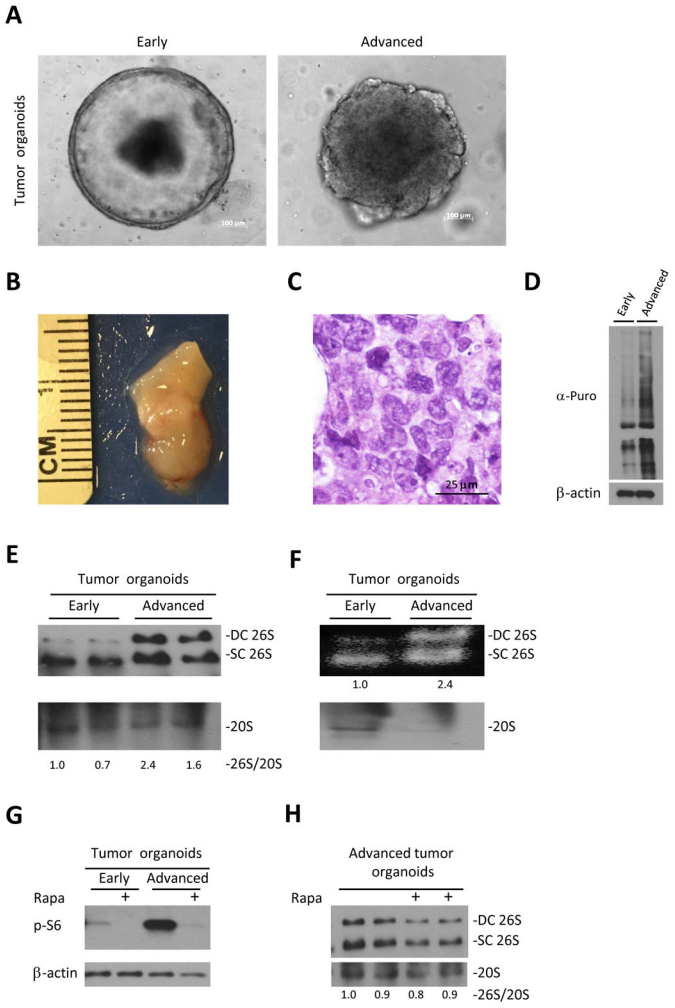

Figure 4. Progression of the tumor organoids is associated with increase in assembly of 26S

A. Representative images of early and advanced organoids originating from large bowel tumors of $APC^{min/+}$ mice. **B.** Representative picture of xenograft deriving from advanced tumor organoids, 6 weeks after injection to NSG mice. **C.** H&E staining of advanced tumor organoids xenograft reveals cells with different nuclear size and shape, prominent nucleoli with almost no gland formation characteristic of malignant cells. **D.** Large bowel early and advanced tumor organoids of $APC^{min/+}$ mice were cultured in the presence of 4 uM Puromycin for 30 min. Puromycin incorporation, detected by anti-puromycin antibody, shows increase in translation with tumor progression.

E. Native gel electrophoresis of tumor organoids shown in **A.** demonstrates increase of 26S assembly in advanced tumor organoids. **26S and 20S** were detected by anti-RPT1 and anti-Alpha7 antibodies respectively. **F.** In gel suc-LLVY-AMC activity assay (no SDS) of tumor organoids shown in **A**. shows increased in the amount of active 26S proteasomes in advanced tumor organoids at expense of unassembled 20S. **G.** Western blot of organoids cultured with/without 300nM of Rapamycin (Rapa) for 6 hours shows activation of mTORC1 in advanced organoids as expressed in the levels of pS6 **H.** Native gel electrophoresis of advanced tumor organoids cultured with/without 300nM of Rapamycin

(Rapa) for 6 hours demonstrates no effect of mTORC1 inhibition on 26S assembly. **DC 26S** – Double capped 26S, **SC 26S** – Single capped 26S. Densitometry was performed using ImgeJ. 26S proteasome assembly status(26S/20S) is reported as the relative intensity of 26S (DC+SC) divided by intensity of 20S.

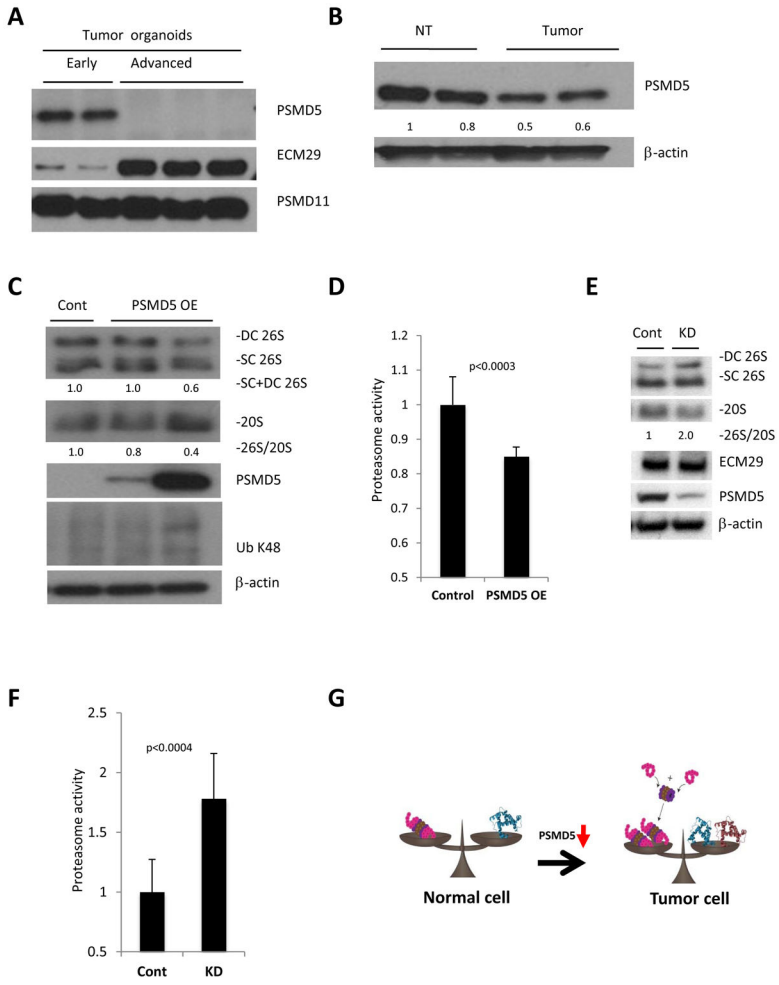

Figure 5. PSMD5 is a possible mediator of enhanced proteasome assembly in tumors with high protein turnover

A. Western blot analysis of potential regulators of 26S assembly identified in the RNA-seq, showing significant reduction of PSMD5 and elevation of ECM29 in advanced organoids, with no change in PSMD11. **B.** Western blot of large bowel normal tissue and tumors from $APC^{min/+}$ mice shows reduced levels of PSMD5 in intestinal tumors. **C.** Western blot analysis following native gel electrophoresis (two upper panels) and SDS-Page (3 lower panels) of advanced organoids. Over-expression of PSMD5 leads to reduced assembly of 26S proteasomes and accumulation of poly-ubiquitinated proteins. **D**. Proteasome activity of cell lysates of advanced tumor organoids overexpressing PSMD5 and their controls. Values obtained for controls were set as 1. The error bars represent the standard deviation from triplicate measurements of 3 biological repetitions. Statistical analysis was performed with *t*-test. **E.** Western blot analysis following native gel electrophoresis (two upper panels) and SDS-Page (3 lower panels) of HT-29 cells transfected with control siRNA (Cont) or PSMD5 siRNA (KD). F. Proteasome activity of HT-29 cells transfected with control siRNA (Cont) or PSMD5 siRNA (KD). Values obtained for controls were set as 1. The error bars represent the standard deviation from average of 12 biological replicates. Statistical analysis was performed with a *t*-test. **G.** A model of enhanced 26S proteasome assembly in cancer cells.

Upon malignant transformation tumor cells start to synthesize more protein. In order to degrade these excess proteins, tumor cells stimulate assembly of 26S proteasomes by inhibition of PSMD5 expression. **DC 26S** – Double capped 26S, **SC 26S** – Single capped 26S. **26S and 20S** were detected by anti-RPT1 and anti-Alpha7 antibodies, respectively. Densitometry was performed using ImgeJ. 26S proteasome assembly status (26S/20S) is reported as the relative intensity of 26S (DC+SC) divided by intensity of 20S.

Table 1

	Log2FoldChange
Psmd5	−5.9
Psmb11	−1.9
Psmg3	−1.8
Psmb8	−1.7
Psmd9	−1.2
Psma7	1.1
Psmd4	1.1
Psmc1	1.2
Psma5	1.4
Psmd14	1.5
Psmf1	1.5
Psmd10	1.5
Psmd11	1.7
Psmb9	1.8
ECM29	1.9
Psmb7	1.9
Psma4	2.7